Applied Soft Computing Journal 74 (2019) 621–633

Contents lists available at ScienceDirect

Applied Soft Computing Journal

journal homepage: www.elsevier.com/locate/asoc

MOEA/D with angle-based constrained dominance principle for constrained multi-objective optimization problems

Zhun Fan [a,b], Yi Fang [a,1], Wenji Li [a,1], Xinye Cai [c,d,*], Caimin Wei [e], Erik Goodman [f]

[a] Department of Electronic Engineering, Shantou University, Guangdong, 515063, China
[b] Key Lab of Digital Signal and Image Processing of Guangdong Province, Guangdong, 515063, China
[c] College of Computer Science and Technology, Nanjing University of Aeronautics and Astronautics, Jiangsu, 210016, China
[d] Collaborative Innovation Center of Novel Software Technology and Industrialization, Nanjing 210023, China
[e] Department of Mathematics, Shantou University, Guangdong, 515063, China
[f] BEACON Center for the Study of Evolution in Action, Michigan State University, East Lansing, MI, USA

HIGHLIGHTS

- The proposed MOEA/D-ACDP utilizes the angle information to maintain the diversity.
- MOEA/D-ACDP enhances convergence to the PF by exploring infeasible regions.
- MOEA/D-ACDP is significantly better than the other six CMOEAs on the benchmark problems.

ARTICLE INFO

Article history:
Received 13 February 2018
Received in revised form 6 September 2018
Accepted 15 October 2018
Available online 22 October 2018

Keywords:
Constraint-handling mechanism
Angle-based constrained dominance principle (ACDP)
Constrained multi-objective evolutionary algorithms (CMOEAs)

ABSTRACT

This paper proposes a novel constraint-handling mechanism, namely the angle-based constrained dominance principle (ACDP), to solve constrained multi-objective optimization problems (CMOPs). In this work, the mechanism of ACDP is embedded in a decomposition-based multi-objective evolutionary algorithm (MOEA/D). ACDP uses the angle information among solutions of a population and the proportion of feasible solutions to adjust the dominance relationship, so that it can maintain good convergence, diversity and feasibility of a population, simultaneously. To evaluate the performance of the proposed MOEA/D-ACDP, fourteen benchmark instances and an engineering optimization problem are studied. Six state-of-the-art CMOEAs, including C-MOEA/D, MOEA/D-CDP, MOEA/D-Epsilon, MOEA/D-SR, NSGA-II-CDP and SP, are compared. The experimental results illustrate that MOEA/D-ACDP is significantly better than the other six CMOEAs on these benchmark problems and the real-world case, which demonstrates the effectiveness of ACDP.

1. Introduction

Multi-objective optimization problems (MOPs) involve the optimization of more than one objective function. In the real world, many optimization problems involve a number of constraints and multiple conflicting objectives. In general, a CMOP can be described mathematically as follows:

$$\begin{cases} \text{minimize} & \mathbf{F}(\mathbf{x}) = (f_1(\mathbf{x}), \ldots, f_m(\mathbf{x}))^T \\ \text{subject to} & g_i(\mathbf{x}) \geq 0, i = 1, \ldots, q \\ & h_j(\mathbf{x}) = 0, j = 1, \ldots, p \\ & \mathbf{x} \in \mathbb{R}^n \end{cases} \tag{1}$$

where $F(\mathbf{x}) = (f_1(\mathbf{x}), f_2(\mathbf{x}), \ldots, f_m(\mathbf{x}))^T \in \mathbb{R}^m$ is an m-dimensional objective vector, $g_i(\mathbf{x}) \geq 0$ is the ith inequality constraint, and $h_j(\mathbf{x}) = 0$ is the jth equality constraint. $\mathbf{x} \in \mathbb{R}^n$ is an n-dimensional decision vector. The feasible region S is defined as the set $\{\mathbf{x} | g_i(\mathbf{x}) \geq 0, i = 1, \ldots, q \text{ and } h_j(\mathbf{x}) = 0, j = 1, \ldots, p\}$.

In CMOPs, there are usually more than one constraint. To capture the degree of constraint violation, these constraints are commonly summarized into a scalar value as follows:

$$\phi(\mathbf{x}) = \sum_{i=1}^{q} |\min(g_i(\mathbf{x}), 0)| + \sum_{j=1}^{p} |h_j(\mathbf{x})| \tag{2}$$

When $\phi(\mathbf{x}) = 0$, the solution $\mathbf{x}$ is feasible; otherwise it is infeasible.

For any two feasible solutions $\mathbf{x}^a \in \mathbb{R}^n$ and $\mathbf{x}^b \in \mathbb{R}^n$ of a CMOP, it can be said that $\mathbf{x}^a$ dominates $\mathbf{x}^b$ if the following condition is met:

$$\forall i\, f_i(\mathbf{x}^a) \leq f_i(\mathbf{x}^b) \text{ and } \exists j\, f_j(\mathbf{x}^a) < f_j(\mathbf{x}^b) \tag{3}$$

where $i, j \in \{1, 2, \ldots, m\}$. If there exists a solution $\mathbf{x}^* \in S$ that is not dominated by any other solution in S, $\mathbf{x}^*$ can be said to be a

* Corresponding author at: College of Computer Science and Technology, Nanjing University of Aeronautics and Astronautics, Jiangsu, 210016, China.
E-mail address: xinye@nuaa.edu.cn (X. Cai).

[1] The two authors make equal contributions to this work.

https://doi.org/10.1016/j.asoc.2018.10.027
1568-4946/

Pareto optimal solution. The set of all Pareto optimal solutions is called a Pareto set (PS). The set of the vectors in the objective set to which the PS maps is called the Pareto front (PF), which can be defined in the form $PF = \{F(\mathbf{x})| \mathbf{x} \in PS\}$.

Maintaining a balance among convergence, diversity and feasibility of a population is very critical when solving CMOPs. There are two basic aspects of maintaining the balance of these three metrics in constrained MOEAs (CMOEAs). One is the multi-objective optimization method and the other is the constraint-handling technique. Multi-objective evolutionary algorithms (MOEAs) are widely used to solve MOPs, because MOEAs can, in a single run, evolve a set of non-dominated solutions that approach the global optimum and are well distributed. According to the selection strategy used in the evolutionary process, MOEAs can be classified into three different types. The first type is the dominance-based MOEA, which uses a selection strategy based on Pareto domination. A popular MOEA of this type is NSGA-II [1], which adopts a non-dominated sorting and elitism-preserving strategy. Other representative dominance-based algorithms include NSGA [2], MOGA [3], SPEA [4], PAES-II [5], SPEA-II [6] and NPGA [7]. The second type is the decomposition-based MOEA. A representative example is MOEA/D [8], which decomposes an MOP into a number of single-objective optimization problems(SOPs). In recent years, decomposition-based MOEAs have attracted much attention, and many variants of MOEA/D have been proposed, including MOEA/D-DE [9], MOEA/D-M2M [10], EAG-MOEA/D [11], MOEA/D-SAS [12] and so on. The third type of MOEA is the indicator-based MOEA. A classic example of this type is IBEA, which uses a scalar metric index to assist the selection [13]. Other representative examples of this type include SMS-EMOA [14], HypE [15] and FV-MOEA [16].

The constraint-handling technique is the other key component in CMOEAs. In general, constraint-handling methods can be classified into four types. The first type is the feasibility-driven method, which tends to preserve feasible solutions in a population. Coello Coello and Christiansen [17] proposed a simple method, in which infeasible solutions are all ignored during the evolutionary process. Deb et al. proposed a constrained dominance principle (CDP) [18] to compare two arbitrary solutions. CDP has three basic rules: (1) When two feasible solutions are compared, the one dominating the other in terms of objectives is better. (2) When a feasible solution is compared with an infeasible one, the feasible one is better. (3) When two infeasible solutions are compared, the one with a smaller degree of constraint violation is better. Powell and Skolnick [19] proposed a constraint-handling technique named superiority of feasible solution (SF). For an infeasible solution, its fitness is defined as the sum of the objective value of the worst feasible solution (f_{worst}) and the constraint violation $\phi(\mathbf{x})$ of the infeasible solution, whereas the fitness of a feasible solution is simply equal to its objective value. Therefore, feasible solutions are always better than infeasible solutions. The above feasibility-driven constraint-handling methods have not taken full advantage of the useful information contained in the infeasible solutions, which may lead them to become trapped in local optima.

The second type trades off the feasibility and convergence of a population simultaneously. Jimsenez et al. proposed a min–max formulation [20], which drives infeasible solutions to evolve toward feasible ones, and drives the feasible solutions to evolve toward the global optimum. Young proposed a non-dominated ranking method [21] which blends the ranks of a solution in both objective and constraint spaces. Singh proposed an infeasibility-driven evolutionary algorithm (IDEA), which maintains a small proportion of infeasible solutions in the population to improve the convergence [22]. In [23], a stochastic ranking method (SR) was proposed, in which solutions are compared based on objectives or constraints randomly with a probability S_r. Takahama et al. proposed an ϵ constraint-handling method [24]. When the constraint violation of a solution is smaller than ϵ, it is regarded as a feasible solution. In [25], an adaptive ϵ constraint-handling method was proposed. Ning proposed a constrained non-dominated rank based on the constraint violation and Pareto rank [26] to balance the feasibility and convergence. Most constraint-handling methods of this type do not explicitly consider a mechanisms to maintain diversity of the population, especially for solving CMOPs with large infeasible regions.

The third type is the penalty-based method. Woldesenbet et al. proposed an adaptive penalty function, which consists of a distance value and two penalty values [27]. Jan and Zhang proposed a penalty function for MOEA/D. It adopts two types of penalty functions [28]. However, the ideal penalty factors are difficult to set in advance.

The fourth type is the hybrid method, which combines parts of several constraint-handling methods to deal with constraints. Wang et al. proposed the adaptive tradeoff model (ATM) [29]. In ATM, the evolutionary process is classified into three phases. In each phase, a different constraint-handling method is adopted. Qu et al. proposed an ensemble method to deal with constraints [30]. It has several sub-populations, and each sub-population uses a different constraint-handling method.

It can be concluded that most of the existing constraint-handling methods emphasize treating convergence and feasibility during the evolutionary process, while diversity is usually not explicitly considered and well maintained. In this paper, we propose a new constraint-handling method named ACDP, which can maintain good diversity as well as convergence and feasibility of a population simultaneously. The method uses the angle information among solutions of a population and the proportion of feasible solutions to adjust the dominance relationship.

The rest of this paper is organized as follows: Section 2 briefly introduces MOEA/D, NSGA-II and six representative CMOEAs. Section 3 introduces the details of the angle-based constrained dominance principle embedded in MOEA/D. Section 4 gives comprehensive experimental results of the proposed algorithm MOEA/D-ACDP and six other CMOEAs on LIR-CMOPs and the I-beam optimization problem. Finally, conclusions are made in Section 5.

2. Related work

2.1. Decomposition-based CMOEAs

In the original framework of MOEA/D [8], given a series of uniformly distributed weight vectors, a MOP is decomposed into N scalar subproblems (SOPs), and each SOP relates to one solution. In MOEA/D, a set of N uniformly spread weight vectors $\lambda^1, \ldots, \lambda^N$ is initially generated for N subproblems. A weight vector λ^i satisfies the following conditions:

$$\sum_{k=1}^{m} \lambda_k^i = 1 \quad \text{and} \quad \lambda_k^i \geq 0 \quad \text{for each } k \in \{1, \ldots, m\}. \tag{4}$$

There are several approaches to decompose a MOP into a number of scalar optimization subproblems [8,31]. Three decomposition approaches, including the weighted sum [31], Tchebycheff [31] and boundary intersection approaches [8] are commonly used. In this paper, the Tchebycheff decomposition method is used in the MOEA/D framework. The jth subproblem is defined as follows:

$$\text{minimize } g^{te}(\mathbf{x}|\lambda^j, z^*) = \max_{1\leq i\leq m} \left\{ \frac{1}{\lambda_i^j} |f_i(\mathbf{x}) - z_i^*| \right\}$$
$$\text{subject to } \mathbf{x} \in S \tag{5}$$

where $z^* = (z_1^*, \ldots, z_m^*)$ is the ideal point, and $z_i^* = \min\{f_i(\mathbf{x})|\mathbf{x} \in S\}$.

Decomposition-based CMOEAs combine the MOEA/D with different constraint-handling mechanisms. In this paper, we introduce four representative decomposition-based CMOEAs including C-MOEA/D [25], MOEA/D-CDP [32], MOEA/D-Epsilon [33], and MOEA/D-SR [32].

- C-MOEA/D [25] uses a variant of the epsilon constraint-handling technique. In this technique, the epsilon level is set to handle constraints according to the constraint violation and the proportion of feasible solutions in the current population. When comparing any two solutions, if overall constraint violations of the solutions are both less than the epsilon level, the one with a better aggregation value dominates the other. Otherwise, the one with a smaller overall constraint violation dominates the other.
- MOEA/D-CDP [32] uses CDP to judge the dominance relationship between two arbitrary solutions. The comparison between two solutions is based on the following two rules:
  (1) When two feasible solutions are compared, the one with a better aggregation value is better.
  (2) When at least one of two solutions is infeasible, the one with a smaller degree of overall constraint violation is better.
- MOEA/D-Epsilon [33] uses the original epsilon constraint-handling technique. The epsilon level setting can be found in [34]. As the generation counter K increases, the epsilon level dynamically decreases.
- MOEA/D-SR [32] embeds the stochastic ranking method (SR) [23] in MOEA/D to deal with constraints. A threshold parameter $r_f \in [0, 1]$ is set to balance the selection between the objectives and the constraints. When comparing two solutions, if a random number in $[0, 1]$ is less than r_f, the one with a better aggregation value is retained into the next generation. If the random number in $[0, 1]$ is greater than r_f, MOEA/D-SR is similar to MOEA/D-CDP. In the case of $r_f = 0$, MOEA/D-SR is equivalent to MOEA/D-CDP.

2.2. Dominance-based CMOEAs

Currently NSGA-II [1] is a widely used dominance-based MOEA. In NSGA-II, an offspring population Q is generated by genetic operators from the population P at each generation. A fast non-dominated sorting approach is applied on $P \cup Q$. Each individual is assigned to a non-dominated rank. Solutions in the first k ranks are selected into P', until the number of solutions in P' is greater than or equal to the population size NP. If the size of P' is greater than NP, solutions in the kth rank are first removed from P'. Then, solutions in the kth rank are sorted based on crowding distances in descending order, and the first $|NP - P'|$ solutions are added to P' to make sure that the size of P' is equal to NP.

Dominance-based CMOEAs select the next generation based on the fast non-dominated sorting approach. Two representative examples include NSGA-II-CDP [1] and SP [27]. In NSGA-II-CDP [1], the CDP method is adopted to judge the dominance relationship between any two individuals. In SP [27], a CMOP is transformed into an unconstrained MOP by using a penalty function. The value of the penalty function is self-adaptively changing according to the feasibility fraction of the current population. The population is sorted based on non-dominated sorting [1] on the transformed objectives during the evolutionary process.

3. MOEA/D with angle-based constrained dominance principle

In this section, the definition of the proposed ACDP and the effectiveness of this mechanism in MOEA/D are detailed.

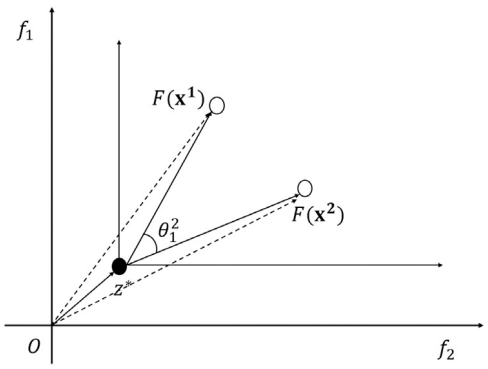

Fig. 1. Illustration of the angle between $\mathbf{x}^1$ and $\mathbf{x}^2$.

3.1. Angle-based constrained dominance principle

In the CDP approach [1], with its three basic rules, the overall constraint violation is the most important factor during the evolutionary process, and some useful information in the infeasible regions tends to be ignored.

The angle between two solutions in the objective space can be used to measure their similarity [35]. Compared with other Euclidean distance metrics, the angle information is easier for normalization [36]. In this paper, we propose an angle-based constrained dominance principle(ACDP) to deal with constraints.

The definition of the angle between any two solutions $\mathbf{x}^1$ and $\mathbf{x}^2$ is given as follows:

$$angle(\mathbf{x}^1, \mathbf{x}^2, z^*) = \arccos\left(\frac{(\mathbf{F}(\mathbf{x}^1) - z^*)^T \cdot (\mathbf{F}(\mathbf{x}^2) - z^*)}{\|\mathbf{F}(\mathbf{x}^1) - z^*\| \cdot \|\mathbf{F}(\mathbf{x}^2) - z^*\|}\right) \tag{6}$$

where $z^* = (z_1^*, \ldots, z_m^*)$ is the ideal point, and $z_i^* = \min\{f_i(\mathbf{x}) | \mathbf{x} \in S\}$. $\|\cdot\|$ is the two-norm of a vector.

As shown in Fig. 1, given any two solutions $\mathbf{x}^1$ and $\mathbf{x}^2$, the angle between them in the objective space is θ_1^2. Obviously, the angle between any two solutions is less than or equal to $\pi/2$, which means that the range of angle between any two solutions belongs in $[0, \pi/2]$.

Given any two solutions $\mathbf{x}^1$ and $\mathbf{x}^2$, a threshold angle θ, a random number r and a parameter p_f ($\frac{\text{Number of Feasible Solutions}}{\text{Population Size}}$) which denotes the proportion of feasible solutions in the current population, the ACDP is defined as follows:

1. If both solutions are feasible, given one solution dominates the other, the one dominating the other is better; otherwise, they are incomparable.
2. If there is at least one infeasible solution and $angle(\mathbf{x}^1, \mathbf{x}^2, z^*) \leq \theta$, the one with a smaller constraint violation dominates the other.
3. When there is at least one infeasible solution and $angle(\mathbf{x}^1, \mathbf{x}^2, z^*) > \theta$, if $r < p_f$, and given one solution dominates the other, the one dominating the other is better; otherwise, they are incomparable.

3.2. ACDP in the framework of MOEA/D

As we know, MOEA/D uses the value of the decomposition function of a solution in the updating of its neighbors. In order to use ACDP to handle constraints in the framework of MOEA/D, here we provide a version of ACDP which is suitable to the algorithm.

Given a subproblem with a weight vector λ, for two solutions $\mathbf{x}^1$ and $\mathbf{x}^2$, their overall constraint violations are ϕ^1 and ϕ^2. It is worth noting that $\phi^1 \geq 0, \phi^2 \geq 0$. The aggregation values of $\mathbf{x}^1$ and $\mathbf{x}^2$

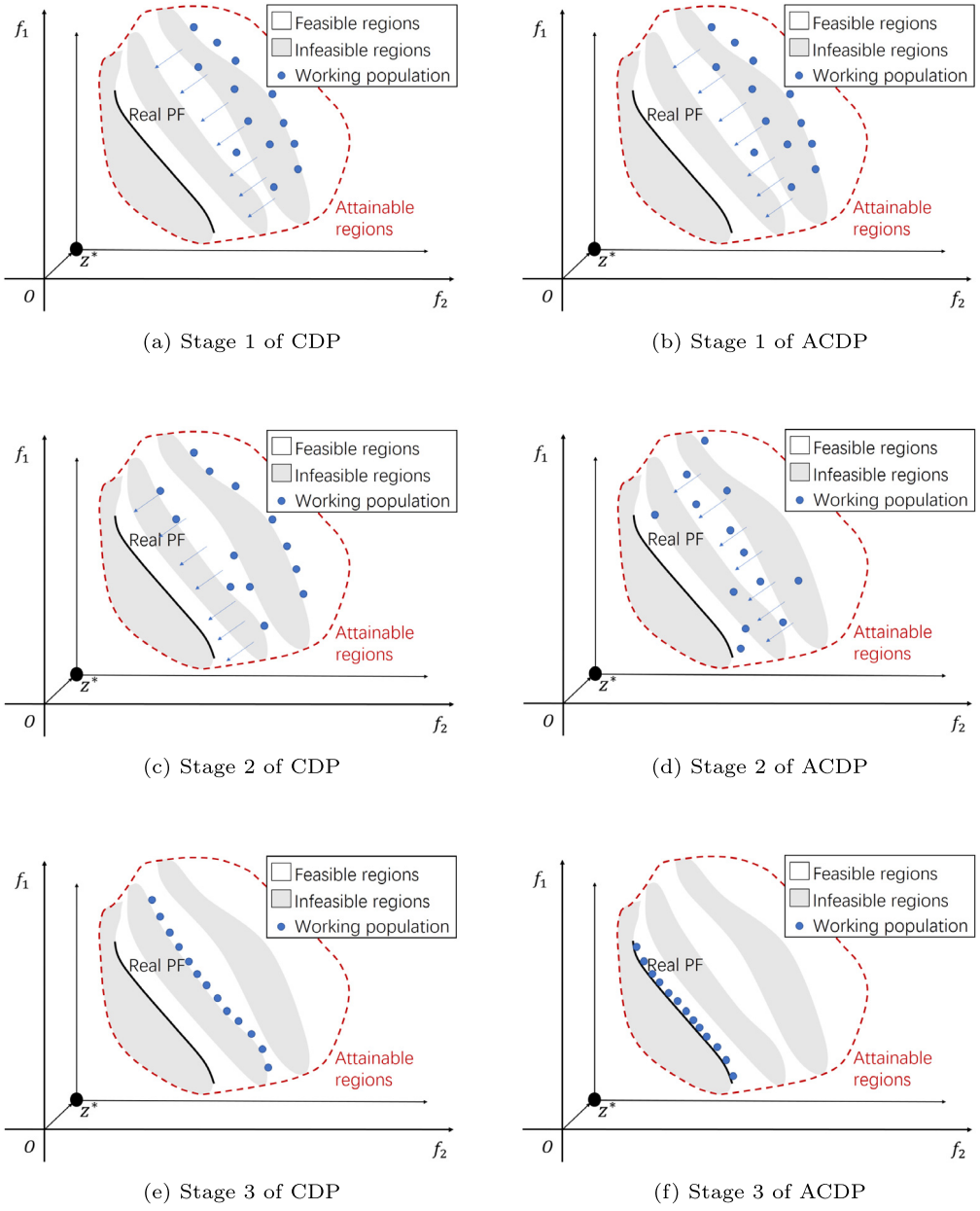

(a) Stage 1 of CDP (b) Stage 1 of ACDP

(c) Stage 2 of CDP (d) Stage 2 of ACDP

(e) Stage 3 of CDP (f) Stage 3 of ACDP

Fig. 2. Illustrations of the evolutionary process of MOEA/D with CDP and ACDP.

on the subproblem sp are $g^{te}(\mathbf{x}^1|\lambda, z^*)$ and $g^{te}(\mathbf{x}^2|\lambda, z^*)$. The ACDP dominance $\preceq_\theta$ in the framework of MOEA/D is defined as follows:

$$\mathbf{x}^1 \preceq_\theta \mathbf{x}^2 \Leftrightarrow \begin{cases} \textbf{Rule 1} \text{ if } \phi^1 = \phi^2 = 0: \\ \quad g^{te}(\mathbf{x}^1|\lambda, z^*) < g^{te}(\mathbf{x}^2|\lambda, z^*); \\ \textbf{Rule 2} \text{ if } \phi^1 + \phi^2 > 0 \text{ and } angle(\mathbf{x}^1, \mathbf{x}^2, z^*) \le \theta: \\ \quad \phi^1 < \phi^2; \\ \textbf{Rule 3} \text{ if } \phi^1 + \phi^2 > 0 \text{ and } angle(\mathbf{x}^1, \mathbf{x}^2, z^*) > \theta: \\ \quad r < p_f \text{ and } g^{te}(\mathbf{x}^1|\lambda, z^*) < g^{te}(\mathbf{x}^2|\lambda, z^*). \end{cases} \tag{7}$$

where θ is a threshold parameter, which is defined by users. In Eq. (7), the constraint-handling method ACDP is equivalent to CDP [1] when $\theta \ge \frac{\pi}{2}$. The reason is that the maximum value of $angle(\mathbf{x}^1, \mathbf{x}^2, z^*)$ is $\frac{\pi}{2}$. As a result, the value of $angle(\mathbf{x}^1, \mathbf{x}^2, z^*)$ is always less than or equal to θ when $\theta \ge \frac{\pi}{2}$. In the case of $\phi^1 < \phi^2$ in Eq. (7), the second rule can be always met, but the third rule can never be fulfilled. Thus, Eq. (7) can be transformed into Eq. (8) when $\theta \ge \frac{\pi}{2}$, which is the same as CDP. Note that Rule 2 of Eq. (7) can be decomposed into two sub-rules. The first sub-rule is that when a feasible solution is compared with an infeasible one, the feasible one is better, which is the same as the second rule of CDP. The second sub-rule is that when two infeasible solutions are compared, the one with a smaller constraint violation is better, which corresponds to the third rule of CDP.

$$\mathbf{x}^1 \preceq_\theta \mathbf{x}^2 (\theta \ge \frac{\pi}{2}) \Leftrightarrow \begin{cases} \textbf{Rule 1} \text{ if } \phi^1 = 0,\ \phi^2 = 0: \\ \quad g^{te}(\mathbf{x}^1|\lambda, z^*) < g^{te}(\mathbf{x}^2|\lambda, z^*); \\ \textbf{Rule 2} \text{ if } \phi^1 + \phi^2 > 0: \\ \quad \phi^1 < \phi^2. \end{cases} \tag{8}$$

In Rule 1 of ACDP, when these two solutions are both feasible, the solution with a lower aggregation value dominates the other, which is similar to the first rule of CDP.

When at least one of $\mathbf{x}^1$ and $\mathbf{x}^2$ is infeasible, CDP only compares the constraint violations of these two solutions, which makes the diversity of the population difficult to maintain when most of the solutions in the population are infeasible. In contrast, ACDP utilizes additional information to compare the two solutions, which includes both the angle between the two compared solutions in the objective space and the proportion of feasible solutions in the current population (p_f). More details of ACDP in this situation are listed as follows:

- In Rule 2 of ACDP, if the angle between $\mathbf{x}^1$ and $\mathbf{x}^2$ in the objective space is smaller than the parameter θ, ACDP considers that these two solutions are similar and compares them according to their constraint violations. Because these two solutions are similar, based on the framework of MOEA/D, they will be considered to relate to the same subproblem. In this situation, using the constraint violations to compare the two solutions will not cause the loss of the diversity.
- In Rule 3 of ACDP, if the angle between $\mathbf{x}^1$ and $\mathbf{x}^2$ in the objective space is larger than the parameter θ, ACDP considers that these two solutions are dissimilar, and the solution with a lower aggregation value will dominate the other with a probability of p_f. Some infeasible solutions with low aggregation values will have a chance to be selected in the next generation, which may enhance the convergence of the population.
- The probability in Rule 3 of ACDP is set to be the proportion of feasible solutions in the current population. It keeps the balance of the exploration of the population between infeasible regions and feasible regions. When p_f is large, ACDP tends to explore infeasible regions. When p_f is small, ACDP tends to explore feasible regions.

3.3. Effectiveness of ACDP in MOEA/D

The evolutionary process of a CMOEA can be generally divided in three stages according to the status of the population. In the first stage, a population is generated randomly, and most of the individuals are far away from the real PF as shown in Fig. 2(a) and Fig. 2(b).

In the second stage, the population begins to explore the search space. As shown in Fig. 2(c), when using CDP in MOEA/D, the population will be attracted to feasible regions and actually find it difficult to go across infeasible regions. As shown in Fig. 2(d), when ACDP is applied to MOEA/D, the population can maintain its diversity by using angle information. Some individuals can enter infeasible regions, which can help the population to go across infeasible regions effectively. Additionally, ACDP uses the proportion of feasible solutions in the current population in its selection of solutions to retain, which can help to balance the search between feasible and infeasible regions.

In the third stage, the population will converge to boundaries of feasible regions, with most individuals that lie on the boundaries being non-dominated. In contrast, when using CDP, the population tends to get trapped in local optima, because of the difficulty of crossing infeasible regions in the second stage, as shown in Fig. 2(e). Instead, when using ACDP, the population can converge to the real PF more completely, as shown in Fig. 2(f), because the population can maintain its diversity and explore infeasible regions in the second stage.

3.4. The setting of θ

In the early stage of the evolutionary process, population members are usually far from the real PF. To prevent the population from being trapped in a local optimum, the value of θ should be small, to maintain the diversity. Later in the evolutionary process, convergence should be emphasized, so the value of θ should become larger. Based on the above analysis, the value $\theta(k)$ should be dynamically increased with increasing generation counter k. In this paper, a method for setting $\theta(k)$ is proposed as follows:

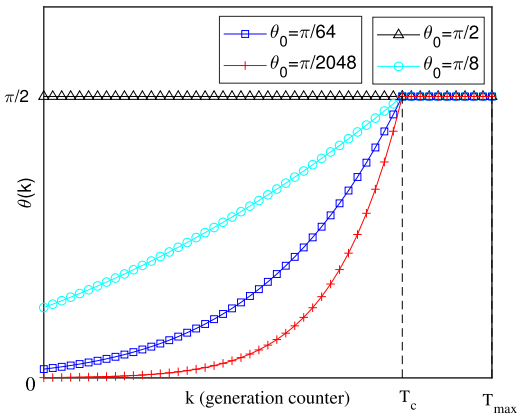

Fig. 3. The changing trends of $\theta(k)$ with different initial values of $\theta(0)$.

$$\theta(k) = \begin{cases} \theta_0 \left(1 + \frac{k}{T_{max}}\right)^{cp}, & 1 \le k \le T_c \\ \frac{\pi}{2}, & T_c < k \le T_{max} \end{cases} \tag{9}$$

where θ_0 is an initial threshold value, N is the size of population and T_{max} is the maximum evolutionary generation. $T_c = \alpha T_{max}$, $\alpha \le 1$, is the final generation for the control of θ. The parameter cp is initialized to $\frac{\log(\pi/(2\theta_0))}{\log(1+\alpha)}$ to make $\theta(k) = \pi/2$ when $k = T_c$.

In Fig. 3, the changing trends of $\theta(k)$ with different initial values of $\theta(0)$ are plotted, which shows that $\theta(k)$ is gradually increasing until $k = T_c$. According to Eq. (9), when the generation counter k reaches T_c, $\theta(k) = \frac{\pi}{2}$. In the early stage of the evolutionary process, $\theta(k)$ increases continuously and slowly, which can help the population to maintain diversity. When k is close to T_c, $\theta(k)$ increases quickly, which helps the population to enhance its convergence. When k reaches T_c, $\theta(k)$ is equal to $\frac{\pi}{2}$, so ACDP is transformed into CDP, which helps the population to maintain feasibility.

3.5. ACDP embedded in MOEA/D

The proposed MOEA/D-ACDP integrates the general framework of MOEA/D and the angle-based constrained dominance principle. The pseudocode of MOEA/D-ACDP is listed in Algorithm 1. Lines 1–5 initialize some parameters in MOEA/D-ACDP. First, a CMOP is decomposed into N subproblems which are associated with weight vectors $\lambda^1, \ldots, \lambda^N$. Then the population P, the initial increasing factor cp, the ideal point z^* and the neighbor indexes $B(i)$ are initialized. Lines 7–11 update the angle threshold value $\theta(k)$. Line 12 updates the proportion of feasible solutions in the current population p_f. Lines 13–23 generate a set of new solutions and update the ideal point z^*. To be more specific, lines 14–21 determine the set of neighboring solutions that may be updated by a newly generated solution $\mathbf{y}^j$. In line 22, the differential evolution (DE) crossover operator is adopted to generate a new solution $\mathbf{y}^j$. Meanwhile, $\mathbf{y}^j$ is further mutated by the polynomial mutation operator. The ideal point z^* is updated in line 23. Lines 24–39 update subproblems. In line 27, the subproblems are updated based on the ACDP approach, for which the detailed pseudocode is listed

Algorithm 1: MOEA/D-ACDP

Input:
N: the number of subproblems.
T_{max}: the maximal generation.
N weight vectors: $\boldsymbol{\lambda}^1, \ldots, \boldsymbol{\lambda}^N$.
T: the size of the neighborhood.
δ: the selecting probability from neighbors.
n_r: the maximal number of solutions replaced by a child.
θ_0, α: the parameters of ACDP method.
Output: NS : a set of feasible non-dominated solutions

1 Decompose a CMOP into N subproblems associated with $\boldsymbol{\lambda}^1, \ldots, \boldsymbol{\lambda}^N$.
2 Generate an initial population $P = \{\mathbf{x}^1, \ldots, \mathbf{x}^N\}$.
3 Initialize cp to $\frac{\log(\pi/(2\theta_0))}{\log(1+\alpha)}$.
4 Initialize the ideal point $z^* = (z_1, \ldots, z_m)$.
5 For each $i = 1, \ldots, N$, set $B(i) = \{i_1, \ldots, i_T\}$, where $\boldsymbol{\lambda}^{i_1}, \ldots, \boldsymbol{\lambda}^{i_T}$ are the T closest weight vectors to $\boldsymbol{\lambda}^i$.
6 **for** $k \leftarrow 1$ **to** T_{max} **do**
7 **if** $k \leq \alpha T_{max}$ **then**
8 Set $\theta(k)$ according to $\theta(k) = \theta_0(1 + \frac{k}{T_{max}})^{cp}$.
9 **else**
10 Set $\theta(k)$ to be equal to $\frac{\pi}{2}$
11 **end**
12 Update pf in the current generation.
13 Generate a random permutation rp from $\{1, \ldots, N\}$.
14 **for** $i \leftarrow 1$ **to** N **do**
15 Generate a random number $r \in [0, 1]$.
16 $j = rp(i)$.
17 **if** $r < \delta$ **then**
18 $S = B(j)$
19 **else**
20 $S = \{1, \ldots, N\}$
21 **end**
22 Generate $\mathbf{y}^j$ through DE and polynomial mutation operators.
23 Update the current ideal point.
24 Set $c = 0$.
25 **while** $c \neq n_r$ and $S \neq \varnothing$ **do**
26 select an index j from S randomly, $S = S \backslash \{j\}$.
27 $result = UpdateSubproblems(\mathbf{x}^j, \mathbf{y}^j, \theta(k), pf)$
28 **if** $result == true$ **then** $c = c + 1$;
29 **end**
30 **end**
31 NS = NondominatedSelect($NS \bigcup P$)
32 **end**

in Algorithm 2. At the end of each generation, non-dominated solutions (NS) in the population are selected to update the external archive based on non-dominated sorting in line 31.

In Algorithm 2, the algorithm updates a subproblem in terms of Eq. (7). Lines 3–7 denote that when two feasible solutions $\mathbf{x}^j$ and $\mathbf{y}^j$ are compared, the one with a better aggregation value is selected. Lines 9–13 denote that when at least one of two solutions $\mathbf{x}^j$ and $\mathbf{y}^j$ is infeasible, if the angle between them in the objective space is lower than θ, the solution with a lower constraint violation is selected. Lines 15–20 denote that when at least one of two solutions $\mathbf{x}^j$ and $\mathbf{y}^j$ is infeasible, if the angle between them in the objective space is larger than θ, the solution with a lower aggregation value will be selected with a probability of p_f.

Algorithm 2: Subproblem Update

1 **Function** $result$ = $UpdateSubproblems(\mathbf{x}^j, \mathbf{y}^j, \theta(k), pf)$
2 $result = false$
3 **if** $\phi(\mathbf{y}^j) = 0$ and $\phi(\mathbf{x}^j) = 0$ **then**
4 **if** $g^{te}(\mathbf{y}^j|\lambda^j, z^*) \leq g^{te}(\mathbf{x}^j|\lambda^j, z^*)$ **then**
5 $\mathbf{x}^j = \mathbf{y}^j$
6 $result = true$
7 **end**
8 **else**
9 **if** $angle(\mathbf{F}(\mathbf{y}^j), \mathbf{F}(\mathbf{x}^j), z^*) < \theta(k)$ **then**
10 **if** $\phi(\mathbf{y}^j) < \phi(\mathbf{x}^j)$ **then**
11 $\mathbf{x}^j = \mathbf{y}^j$
12 $result = true$
13 **end**
14 **else**
15 **if** $rand() < p_f$ **then**
16 **if** $g^{te}(\mathbf{y}^j|\lambda^j, z^*) \leq g^{te}(\mathbf{x}^j|\lambda^j, z^*)$ **then**
17 $\mathbf{x}^j = \mathbf{y}^j$
18 $result = true$
19 **end**
20 **end**
21 **end**
22 **end**
23 **return** $result$
24 **end**

4. Experimental study

4.1. Test instances LIR-CMOPs

To evaluate the performance of the proposed MOEA/D-ACDP, 14 constrained multi-objective test problems with large infeasible regions in the objective space are used [37,38]. The general characteristic of LIR-CMOPs is that their real PFs are blocked by a number of large infeasible regions, and thus hard to find during an evolutionary process. Their constraint functions are comprised of controllable shape functions and distance functions [39]. More specifically, the shape functions are used to make the PF shapes convex or concave, while the distance functions are used to adjust the convergence difficulty for CMOEAs.

4.2. Real-world engineering optimization: I-beam

To evaluate the performance of MOEA/D-ACDP for solving real world optimization problems, an engineering optimization problem with two conflicting objectives is studied.

As defined in [40], the I-beam optimization problem shown in Fig. 4 is a bi-objective constrained optimization problem which needs to minimize the following objectives simultaneously:

1. Cross-sectional area of the beam;
2. Static deflection of the beam for the displacement under force P.

The decision variable vector of the problem is $\mathbf{x} = [x_1, x_2, x_3, x_4]^T$, which is in units of centimeters. The range for each decision variable is listed as follows: $10 \leq x_1 \leq 80$, $10 \leq x_2 \leq 50$, $0.9 \leq x_4 \leq 5$, $0.9 \leq x_4 \leq 5$. Some given parameter settings are listed as follows:

1. Permissible bending stress of the beam's material: $k_g = 1.6$ kN/cm^2.
2. Young's Modulus of Elasticity: $E = 2 \times 10^4$ kN/cm^2.
3. Maximal bending forces: $P = 600$ kN and $Q = 50$ kN.
4. The length of the I-beam: $l = 200$ cm

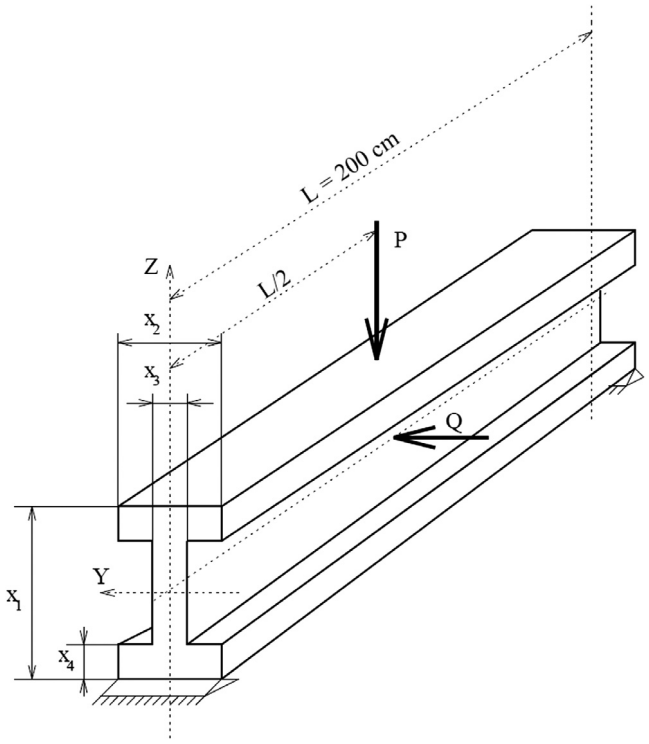

Fig. 4. The geometry modeling of I-Beam.

The I-beam optimization problem considered in this paper is defined as follows:

$$\begin{cases} \text{minimize} \quad f_1(\mathbf{x}) = 2x_2x_4 + x_3(x_1 - 2x_4) \\ \text{minimize} \quad f_2(\mathbf{x}) = \dfrac{Pl^3}{48EI} \\ \text{subject to} \quad c(\mathbf{x}) = k_g - \dfrac{M_y}{W_y} - \dfrac{M_z}{W_z} \end{cases} \tag{10}$$

where I is the inertia coefficient which can be calculated by Eq. (11).

$$I = \frac{x_3(x_1 - 2x_4)^3 + 2x_2x_4[4{x_4}^2 + 3x_1(x_1 - 2x_4)]}{12}. \tag{11}$$

The values of M_y and M_z are 30,000 kN cm and 2500 kN cm, respectively.

The section modulus can be calculated by Eqs. (12) and (13).

$$W_y = \frac{x_3(x_1 - 2x_4)^3 + 2x_2x_4[4{x_4}^2 + 3x_1(x_1 - 2x_4)]}{6x_1} \tag{12}$$

$$W_z = \frac{(x_1 - 2x_4){x_3}^3 + 2x_4{x_2}^3}{6x_2} \tag{13}$$

To study the landscape in the objective space of the I-beam optimization problem, 1,000,000 sampling solutions are generated, where 850,000 solutions are generated randomly, and the other 150,000 solutions are generated by MOEA/D-ACDP. In Fig. 5, it is observed that there exist a few infeasible regions in the objective space for the I-beam optimization problem (the proportion of feasible solutions among all sampled solutions $p = 0.5339$, which means that nearly half of the selected points are infeasible).

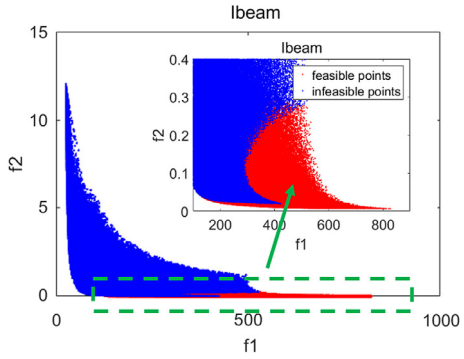

Fig. 5. The distribution of the I-Beam problem.

4.3. Experimental settings

To evaluate the performance of the proposed MOEA/D-ACDP, it is compared with six popular CMOEAs (C-MOEA/D, MOEA/D-CDP, MOEA/D-Epsilon, MOEA/D-SR, NSGA-II-CDP and SP), using a differential evolution (DE) crossover operator. They are tested on LIR-CMOP1-14 and the I-beam optimization problem. The detailed parameters are listed as follows:

1. Polynomial mutation probability $Pm = 1/n$ (n is the number of decision variables) and its distribution index is set to 20. For the DE operator, $CR = 1.0, f = 0.5$.
2. Population size: $N = 300$. Neighborhood size: $T = 30$.
3. Stopping condition: each algorithm is run 30 times independently, and stops when 150,000 function evaluations are reached.
4. Probability of selecting individuals in the neighborhood: $\delta = 0.9$.
5. The maximal number of solutions replaced by a child: $nr = 2$.
6. Parameter setting in MOEA/D-ACDP: $\alpha = 0.8$ and $\theta_0 = \frac{\pi}{2N}$.
7. Parameter setting in MOEA/D-Epsilon: $T_c = 400, cp = 2$ and $\theta = 0.05$ N.
8. Parameter setting in MOEA/D-SR: $S_r = 0.01$.

4.4. Performance metric

To measure the performance of MOEA/D-ACDP, C-MOEA/D, MOEA/D-CDP, MOEA/D-Epsilon, MOEA/D-SR, NSGA-II-CDP and SP, two widely used metrics are employed: inverted generational distance (*IGD*) [41] and hypervolume (*HV*) [4]. Their definitions are as follows.

- **Inverted Generational Distance** (*IGD*):

IGD is a metric which evaluates the performance related to convergence and diversity simultaneously. Let P^* be a set of uniformly distributed points in the ideal PF. Let A denote an approximate PF achieved by a certain CMOEA. The metric *IGD* that represents average distance from P^* to A is defined as:

$$\begin{cases} IGD(P^*, A) = \dfrac{\sum_{y^* \in P^*} d(y^*, A)}{|P^*|} \\ d(y^*, A) = \min_{y \in A}\{\sqrt{\sum_{i=1}^{m}(y_i^* - y_i)^2}\} \end{cases} \tag{14}$$

In our experiment, for CMOPs with two objectives, 1000 points are sampled uniformly from the PF to constitute P^*. For CMOPs with three objectives, 10,000 points are sampled uniformly from the PF to constitute P^*. A smaller *IGD* represents better performance with respect to both diversity and convergence.

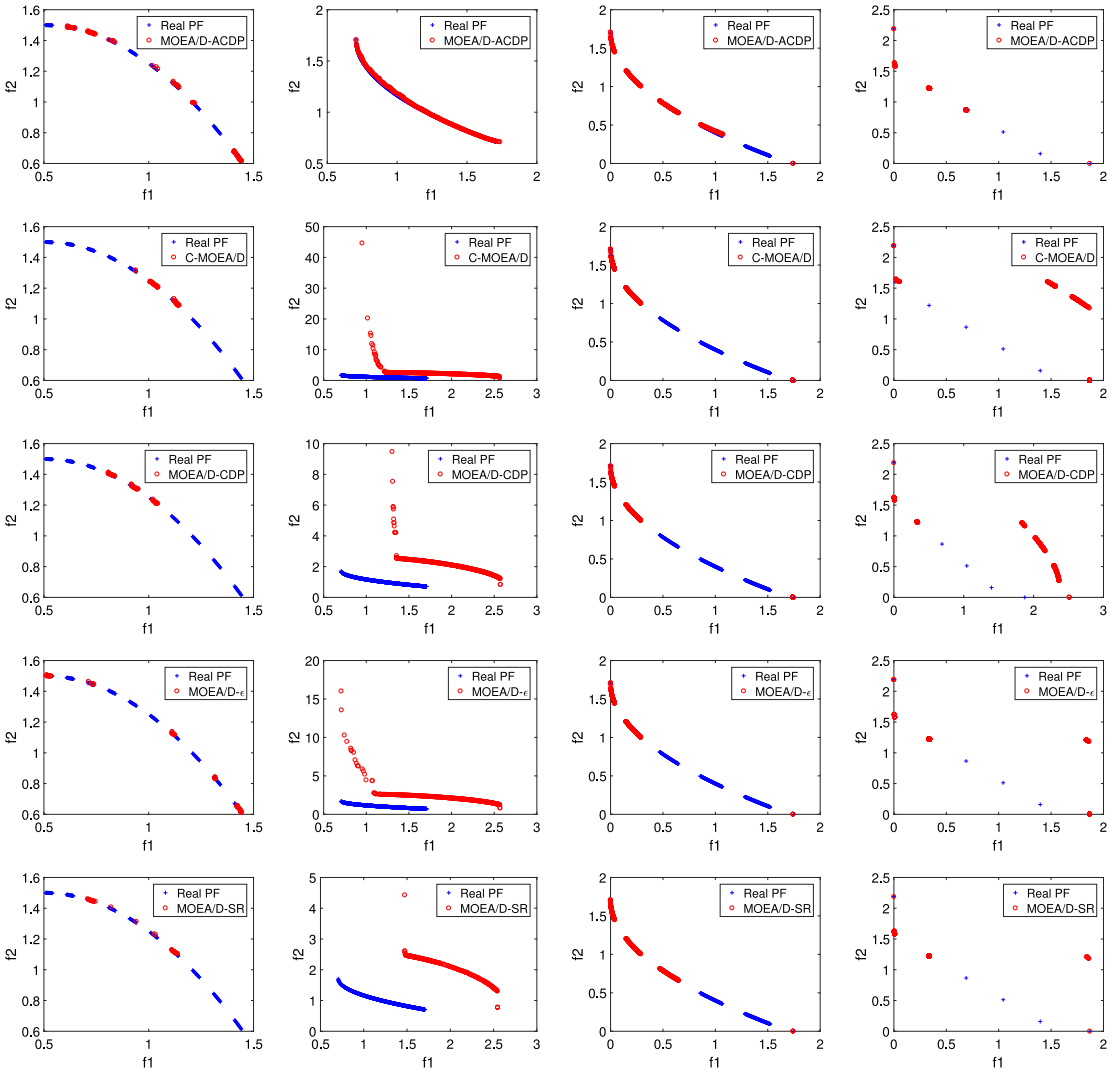

Fig. 6. The non-dominated solutions achieved by MOEA/D-ACDP, C-MOEA/D, MOEA/D-CDP, MOEA/D-Epsilon and MOEA/D-SR with the median *IGD* in 30 independent runs for LIR-CMOP3, LIR-CMOP5, LIR-CMOP10 and LIR-CMOP11.

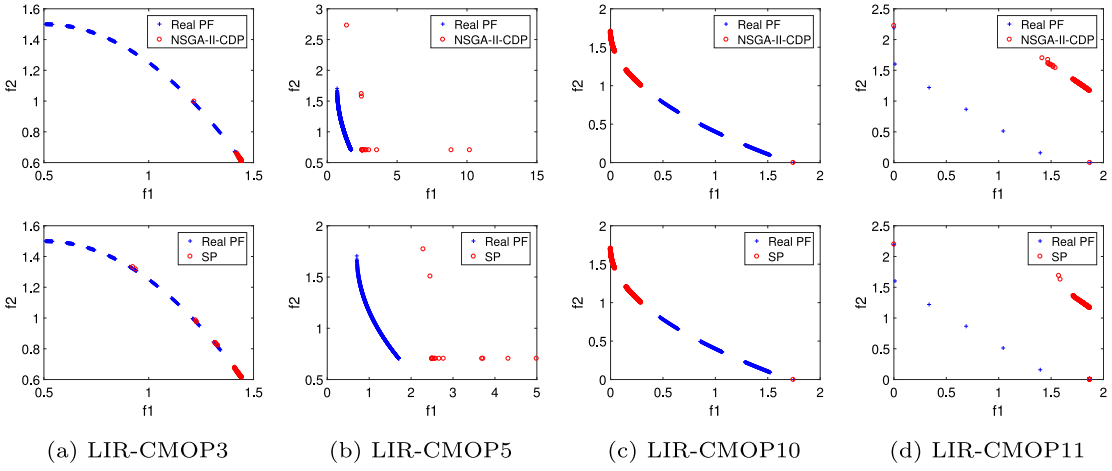

Fig. 7. The non-dominated solutions achieved by NSGA-II-CDP and SP with the median *IGD* in 30 independent runs for LIR-CMOP3, LIR-CMOP5, LIR-CMOP10 and LIR-CMOP11.

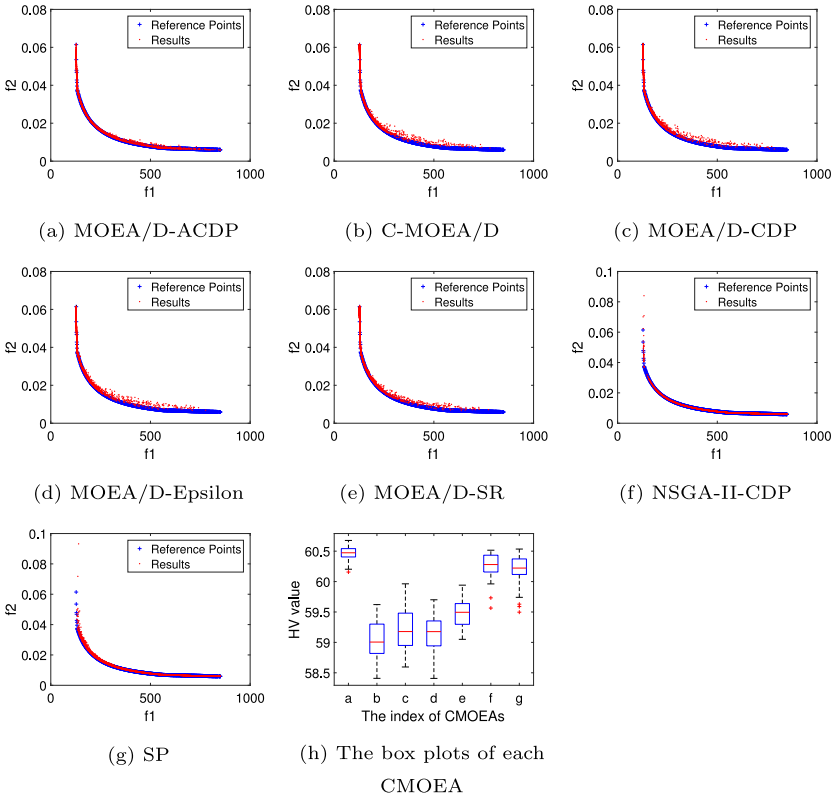

(a) MOEA/D-ACDP (b) C-MOEA/D (c) MOEA/D-CDP

(d) MOEA/D-Epsilon (e) MOEA/D-SR (f) NSGA-II-CDP

(g) SP (h) The box plots of each CMOEA

Fig. 8. The non-dominated solutions achieved by each algorithm during 30 independent runs are plotted in (a)–(g). In (h), the box plots of each CMOEA are plotted.

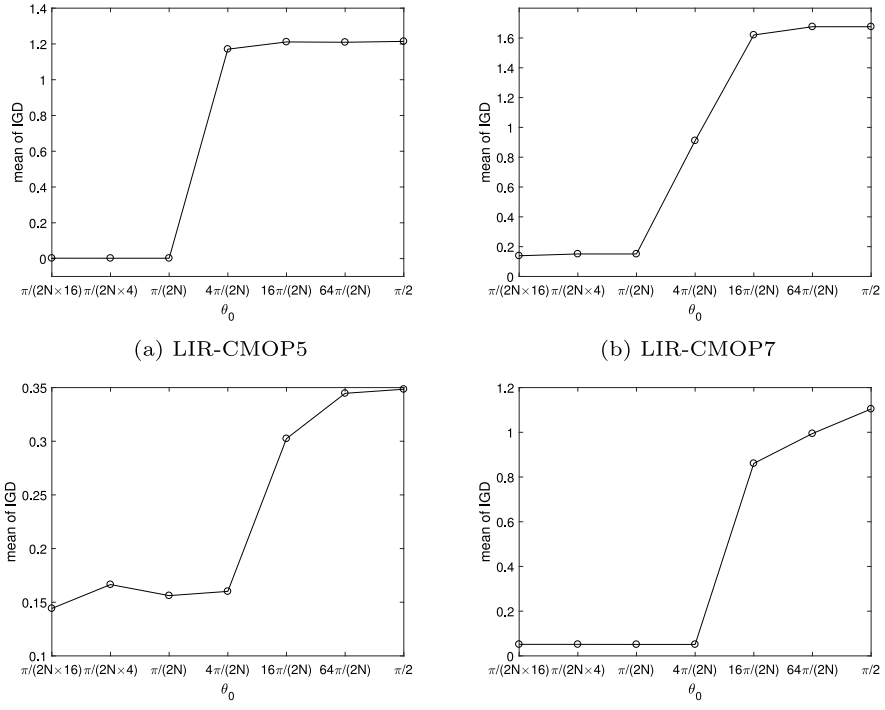

(a) LIR-CMOP5 (b) LIR-CMOP7

(c) LIR-CMOP12 (d) LIR-CMOP14

Fig. 9. Means of IGD by using MOEA/D-ACDP for initial threshold $\theta_0 \in \{\frac{\pi}{2N\times16}, \frac{\pi}{2N\times4}, \frac{\pi}{2N}, \frac{\pi\times4}{2N}, \frac{\pi\times16}{2N}, \frac{\pi\times64}{2N}, \frac{\pi}{2}\}$ on LIR-CMOP5, 7, 12, 14 at 30 independent runs.

Table 1
IGD results of MOEA/D-ACDP and the other six CMOEAs on LIR-CMOP1-14 test instances.

LIR-CMOP		MOEA/D-ACDP	C-MOEA/D	MOEA/D-CDP	MOEA/D-Epsilon	MOEA/D-SR	NSGA-II-CDP	SP
1	mean	5.159E−02	1.591E−01†	1.348E−01†	8.234E−02†	**4.406E−02**	4.376E−01†	1.489E−01†
	std	1.815E−02	3.534E−02	5.996E−02	5.321E−02	3.360E−02	1.071E−01	8.479E−02
2	mean	2.269E−02	1.462E−01†	1.549E−01†	4.708E−02†	**2.057E−02**	3.084E−01†	1.943E−01†
	std	9.418E−03	4.141E−02	2.966E−02	1.339E−02	1.072E−02	9.513E−02	9.688E−02
3	mean	**4.659E−02**	2.309E−01†	2.268E−01†	7.858E−02†	1.529E−01†	4.082E−01†	2.054E−01†
	std	1.850E−02	4.135E−02	4.403E−02	2.978E−02	7.688E−02	1.120E−01	1.296E−01
4	mean	**2.784E−02**	2.080E−01†	2.188E−01†	5.662E−02†	2.038E−01†	3.081E−01†	1.920E−01†
	std	1.477E−02	4.197E−02	3.766E−02	3.366E−02	7.907E−02	7.367E−02	9.019E−02
5	mean	**1.771E−02**	1.162E+00†	1.207E+00†	1.201E+00†	1.123E+00†	1.153E+00†	1.145E+00†
	std	2.965E−02	2.180E−01	1.660E−02	1.963E−02	2.842E−01	2.425E−01	2.473E−01
6	mean	**1.757E−01**	1.265E+00†	1.303E+00†	1.231E+00†	1.175E+00†	1.134E+00†	1.260E+00†
	std	4.129E−02	3.067E−01	2.319E−01	3.602E−01	3.967E−01	4.743E−01	4.769E−01
7	mean	**1.408E−01**	1.620E+00†	1.623E+00†	1.568E+00†	1.136E+00†	4.596E−01†	7.327E−01†
	std	4.385E−02	3.036E−01	2.905E−01	4.101E−01	7.315E−01	4.854E−01	3.714E−01
8	mean	**1.812E−01**	1.607E+00†	1.631E+00†	1.577E+00†	1.369E+00†	6.017E−01†	6.495E−01†
	std	4.854E−02	2.680E−01	2.464E−01	3.767E−01	5.735E−01	3.991E−01	4.664E−01
9	mean	**3.595E−01**	4.981E−01†	4.868E−01†	4.962E−01†	4.813E−01†	5.261E−01†	5.428E−01†
	std	5.345E−02	6.991E−02	5.372E−02	6.987E−02	4.571E−02	1.060E−01	1.083E−01
10	mean	**1.388E−01**	3.775E−01†	3.774E−01†	3.257E−01†	2.821E−01†	4.790E−01†	4.893E−01†
	std	1.148E−01	7.446E−02	6.858E−02	9.833E−02	1.135E−01	1.928E−01	1.501E−01
11	mean	**1.318E−01**	4.422E−01†	4.662E−01†	4.154E−01†	3.489E−01†	6.052E−01†	6.342E−01†
	std	4.487E−02	1.759E−01	1.439E−01	1.508E−01	1.129E−01	9.166E−02	9.894E−02
12	mean	**1.497E−01**	3.597E−01†	3.236E−01†	3.680E−01†	3.012E−01†	4.166E−01†	4.171E−01†
	std	9.985E−03	1.074E−01	1.023E−01	8.664E−02	8.989E−02	4.386E−02	1.011E−01
13	mean	**7.414E−02**	1.266E+00†	1.289E+00†	1.183E+00†	1.093E+00†	1.317E+00†	1.318E+00†
	std	2.727E−03	2.173E−01	6.321E−02	3.456E−01	4.269E−01	1.433E−03	5.009E−02
14	mean	**6.732E−02**	1.235E+00†	1.103E+00†	1.127E+00†	1.143E+00†	1.273E+00†	1.277E+00†
	std	1.918E−03	1.209E−01	3.857E−01	3.329E−01	3.002E−01	2.416E−03	3.608E−02

Wilcoxon's rank sum test at a 0.05 significance level is performed between MOEA/D-ACDP and each of the other six CMOEAs. † and ‡ denote that the performance of the corresponding algorithm is significantly worse than or better than that of MOEA/D-ACDP, respectively. The best mean is highlighted in boldface.

- **Hypervolume** (*HV*):

HV reflects the closeness between the non-dominated set achieved by a CMOEA and the representative PF. A larger *HV* means that the corresponding non-dominated set is closer to the true PF. A *HV* with a larger value represents better performance with respect to both diversity and convergence.

$$HV(S) = VOL\left(\bigcup_{\mathbf{x}\in S}[f_1(\mathbf{x}), z_1^r] \times \cdots [f_m(\mathbf{x}), z_m^r]\right) \tag{15}$$

where $VOL(\cdot)$ is the Lebesgue measure, $\mathbf{z}^r = (z_1^r, \ldots, z_m^r)^T$ is a reference point in the objective space.

Both *IGD* and *HV* metrics are used in the LIR-CMOP instances. For the LIR-CMOPs, the reference point is set as 1.3 times the nadir point of the real PF. As the real PF of the I-beam optimization problem is not known, the *IGD* metric cannot be calculated. Thus, we uses the *HV* metric [4] to measure the performance of the tested CMOEAs on the I-beam optimization problem. In the I-beam optimization case, the reference point is set to $z^r = [1000, 0.08]^T$.

4.5. Discussion of experimental results

4.5.1. Performance evaluation on the LIR-CMOP test instances

The *IGD* values on LIR-CMOP1-14 achieved by seven CMOEAs in 30 independent runs are shown in Table 1. As discussed in Section 4.1, LIR-CMOP1-14 have large infeasible regions in their objective spaces. For LIR-CMOP3-14, MOEA/D-ACDP significantly outperforms the other six compared algorithms in terms of the *IGD* metric. For LIR-CMOP1-2, MOEA/D-ACDP significantly outperforms C-MOEA/D, MOEA/D-CDP, MOEA/D-Epsilon, NSGA-II-CDP and SP, and does not differ significantly from MOEA/D-SR.

The *HV* values on LIR-CMOP1-14 achieved by seven CMOEAs in 30 independent runs are shown in Table 2. For LIR-CMOP3-14, MOEA/D-ACDP significantly outperforms the compared algorithms in terms of the *HV* metric. For LIR-CMOP1, MOEA/D-ACDP significantly outperforms C-MOEA/D, MOEA/D-CDP, NSGA-II-CDP and SP, and is not significantly different from MOEA/D-Epsilon and MOEA/D-SR. For LIR-CMOP2, MOEA/D-ACDP significantly outperforms C-MOEA/D, MOEA/D-CDP, NSGA-II-CDP, NSGA-II-CDP and SP, and is not significantly different from MOEA/D-SR.

Figs. 6(a) and 7(a) show the final external archives achieved by MOEA/D-ACDP and the other six CMOEAs with the median *IGD* values on LIR-CMOP3 during 30 independent runs. It can be seen that MOEA/D-ACDP almost converges to the whole real PF, and it has the best diversity performance among the seven CMOEAs.

In Figs. 6(b) and 7(b), the external archives of each CMOEA with the median *IGD* values on LIR-CMOP5 during 30 independent runs are plotted. It can be seen that MOEA/D-ACDP covers the whole PF. However, the other six CMOEAs are trapped in local optima.

In Figs. 6(c) and 7(c), for LIR-CMOP10, MOEA/D-ACDP has the best performance in terms of convergence. In Figs. 6(d) and 7(d), we can see that MOEA/D-ACDP can discover most parts of the PF on LIR-CMOP11. However, the other six algorithms can find only a few parts of the PF.

4.5.2. Discussion of the experimental results on the LIR-CMOPs

LIR-CMOP3-4 both have several narrow and disconnected feasible regions. If the CDP mechanism is applied, it is very difficult for the population to distribute the individuals among these narrow and disconnected feasible regions. More likely, most individuals will be trapped in one or a few of these feasible regions. However, when ACDP is applied, rule 2 of the ACDP mechanism will

Table 2
HV results of MOEA/D-ACDP and the other six CMOEAs on LIR-CMOP1-14 test instances.

LIR-CMOP		MOEA/D-ACDP	C-MOEA/D	MOEA/D-CDP	MOEA/D-Epsilon	MOEA/D-SR	NSGA-II-CDP	SP
1	mean	1.365E+00	9.499E−01†	1.009E+00†	1.353E+00	**1.376E+00**	9.205E−01†	1.177E+00†
	std	2.493E−02	7.038E−02	1.298E−01	4.417E−02	3.974E−02	8.084E−02	9.278E−02
2	mean	**1.737E+01**	1.395E+01†	1.374E+01†	1.705E+01†	1.736E+01	1.080E+00†	1.321E+00†
	std	1.306E−02	8.154E−02	6.160E−02	1.693E−02	1.890E−02	1.597E−01	2.036E−01
3	mean	**1.188E+00**	7.558E−01†	7.600E−01†	1.184E+00	9.313E−01†	7.925E−01†	9.638E−01†
	std	4.929E−02	5.730E−02	5.809E−02	2.898E−02	1.620E−01	7.920E−02	1.133E−01
4	mean	**1.421E+00**	1.069E+00†	1.051E+00†	1.390E+00†	1.089E+00†	9.025E−01†	1.087E+00†
	std	1.946E−02	6.952E−02	5.462E−02	4.405E−02	1.360E−01	1.084E−01	1.497E−01
5	mean	**1.903E+00**	1.192E−01†	5.805E−02†	5.829E−02†	1.707E−01†	1.774E−01†	1.968E−01†
	std	5.658E−02	3.352E−01	4.042E−04	2.022E−04	4.442E−01	3.498E−01	3.488E−01
6	mean	**1.280E+00**	7.863E−02†	4.312E−02†	1.325E−01†	1.682E−01†	2.700E−01†	2.300E−01†
	std	4.613E−02	3.011E−01	2.362E−01	4.251E−01	4.061E−01	3.622E−01	3.565E−01
7	mean	**3.408E+00**	2.990E−01†	2.886E−01†	4.055E−01†	1.313E+00†	2.921E+00†	2.321E+00†
	std	1.409E−01	6.927E−01	6.348E−01	8.879E−01	1.567E+00	1.078E+00	7.304E−01
8	mean	**3.330E+00**	3.246E−01†	2.695E−01†	3.859E−01†	8.287E−01†	2.505E+00†	2.521E+00†
	std	1.461E−01	5.878E−01	5.297E−01	8.166E−01	1.244E+00	8.397E−01	9.773E−01
9	mean	**4.080E+00**	3.715E+00†	3.755E+00†	3.724E+00†	3.752E+00†	3.513E+00†	3.472E+00†
	std	9.501E−02	2.079E−01	1.600E−01	2.033E−01	1.142E−01	3.230E−01	3.466E−01
10	mean	**3.755E+00**	3.274E+00†	3.268E+00†	3.385E+00†	3.477E+00†	2.903E+00†	2.905E+00†
	std	2.208E−01	1.623E−01	1.416E−01	2.122E−01	2.383E−01	6.628E−01	5.629E−01
11	mean	**5.004E+00**	3.937E+00†	3.842E+00†	4.038E+00†	4.274E+00†	3.167E+00†	3.055E+00†
	std	1.564E−01	6.479E−01	5.507E−01	5.727E−01	4.463E−01	3.863E−01	3.412E−01
12	mean	**6.713E+00**	5.977E+00†	6.134E+00†	6.010E+00†	6.240E+00†	5.771E+00†	5.764E+00†
	std	5.874E−02	3.855E−01	3.617E−01	3.074E−01	2.950E−01	1.601E−01	3.083E−01
13	mean	**7.897E+00**	6.444E−01†	4.728E−01†	1.092E+00†	1.513E+00†	1.601E−01†	3.083E−01†
	std	2.943E−02	1.317E+00	2.689E−01	2.052E+00	2.422E+00	1.420E−02	1.692E−01
14	mean	**8.641E+00**	7.766E−01†	1.627E+00†	1.430E+00†	1.269E+00†	5.810E−01†	6.053E−01†
	std	1.546E−02	6.140E−01	2.473E+00	2.095E+00	1.919E+00	1.683E−02	2.244E−01

Wilcoxon's rank sum test at a 0.05 significance level is performed between MOEA/D-ACDP and each of the other six CMOEAs. † and ‡ denotes that the performance of the corresponding algorithm is significantly worse than or better than that of MOEA/D-ACDP, respectively. The best mean is highlighted in boldface.

enable more well-distributed individuals to survive into the next generation. As a result, MOEA/D-ACDP can help to maintain the diversity of the population during the evolutionary process. From these experimental results, we can also see that MOEA/D-ACDP performs the best on these two test instances.

LIR-CMOP5-14 have some infeasible regions in front of the real PFs, which makes it difficult for CMOEAs to converge to the real PFs. If the CDP mechanism is applied, when feasible individuals attempt to enter the infeasible regions, they will be easily bounced back to the feasible regions, due to rule2 of CDP. However, when ACDP is applied, rule 3 of the ACDP mechanism will be activated when the feasible individuals attempt to enter the infeasible regions (p_f is still high at this stage), which will facilitate a smooth entry because only convergence is considered according to rule 3 of ACDP. Next, when most feasible individuals have entered the infeasible regions, p_f becomes lower and rule 3 is deactivated. In this case, most individuals become non-dominated by each other, because the dominance relationship defined by Eq. (7) does not exist any more. The non-dominance relationship of individuals helps most infeasible ones survive in the offspring generations, and eventually cross the infeasible regions. As a result, using MOEA/D-ACDP can preserve some high-quality infeasible solutions in the population, which can help the population to find the global optimum. From the experimental results in Tables 1 and 2, we can also conclude that MOEA/D-ACDP has the best performance on these ten test instances.

According to the above observations, we can conclude that the proposed MOEA/D-ACDP outperforms the other six CMOEAs. A common feature of the above LIR-CMOPs test instances is that they all have large infeasible regions in their objective spaces. The experimental results demonstrate that the proposed ACDP method can deal with CMOPs well by taking advantage of angle information among solutions of a population and the proportion of feasible solutions.

4.5.3. Performance comparison on the I-beam optimization problem

The experimental results of *HV* values of MOEA/D-ACDP and the six other CMOEAs on the I-beam optimization problem are shown in Table 3. It can be seen that MOEA/D-ACDP significantly outperforms the compared CMOEAs on this engineering problem.

To further study the superiority of the proposed method MOEA/D-ACDP, the non-dominated solutions achieved by each CMOEA during the 30 independent runs are plotted in Fig. 8(a)–(h). The non-dominated set of all the above solutions generates a set of ideal reference points. It is clear that MOEA/D-ACDP has better convergence performance than the other four decomposition-based CMOEAs (C-MOEA/D, MOEA/D-CDP, MOEA/D-Epsilon and MOEA/D-SR). MOEA/D-ACDP has better diversity performance than the two compared dominance-based CMOEAs (NSGA-II-CDP and SP). The box plot of *HV* values of the CMOEAs is shown in Fig. 8(h), which further illustrates that MOEA/D-ACDP outperforms the other six CMOEAs on the I-beam optimization problem.

4.6. Influence of parameter setting in ACDP

There are two critical parameters in ACDP.

(1) T_c, the termination generation for control of $\theta(k)$.
(2) θ_0, the initial value of θ.

In this paper, $T_c = 0.8T_{max}$. This is a default setting of T_c for many algorithms of the same kind in the research community [33,

Table 3
HV results of MOEA/D-ACDP and the other six CMOEAs on the I-Beam optimization problem.

	MOEA/D-ACDP	C-MOEA/D	MOEA/D-CDP	MOEA/D-Epsilon	MOEA/D-SR	NSGA-II-CDP	SP
mean	**6.046E+01**	5.905E+01†	5.921E+01†	5.916E+01†	5.948E+01†	6.026E+01†	6.017E+01†
std	1.096E−01	2.996E−01	3.508E−01	3.246E−01	2.248E−01	2.283E−01	2.775E−01

Wilcoxon's rank sum test at a 0.05 significance level is performed between MOEA/D-ACDP and each of the other six CMOEAs. † and ‡ denote that the performance of the corresponding algorithm is significantly worse than or better than that of MOEA/D-ACDP, respectively. The best mean is highlighted in boldface.

Table 4
Comparison results of MOEA/D-ACDP on LIR-CMOP1-14 with different θ_0 (population size $N = 300$).

$\theta_0 = \frac{\pi}{2N\times16}$	$\theta_0 = \frac{\pi}{2N\times4}$	$\theta_0 = \frac{\pi}{2N}$	$\theta_0 = \frac{\pi\times4}{2N}$	$\theta_0 = \frac{\pi\times16}{2N}$	$\theta_0 = \frac{\pi\times64}{2N}$	$\theta_0 = \frac{\pi}{2}$
3	3	+	1	4	2	2
1	1	−	6	10	12	12
10	10	=	7	0	0	0

Wilcoxon's rank sum test at a 0.05 significance level is performed between MOEA/D-ACDP with $\theta_0 = \frac{\pi}{2N}$ and that with other six initial threshold settings. '+', '−' and '=' denote the number of instances on which MOEA/D-ACDP with the corresponding θ_0 is significantly better/worse/not better and not worse than that with $\theta_0 = \frac{\pi}{2N}$ in terms of the IGD metric, respectively.

42]. We therefore mainly focus on investigating the influence of θ_0 in ACDP.

To analyze the influence of θ_0 setting, we run MOEA/D-ACDP with $\theta_0 = \frac{\pi}{2N\times16}, \frac{\pi}{2N\times4}, \frac{\pi}{2N}, \frac{\pi\times4}{2N}, \frac{\pi\times16}{2N}, \frac{\pi\times64}{2N}, \frac{\pi}{2}$ on LIR-CMOPs for 30 independent runs.

In Table 4, the performance of MOEA/D-ACDP with $\theta_0 = \frac{\pi}{2N\times16}$ and $\theta_0 = \frac{\pi}{2N\times4}$ is similar to that of MOEA/D-ACDP with $\theta_0 = \frac{\pi}{2N}$. When $\theta_0 \geq \frac{\pi\times4}{2N}$, the performance of MOEA/D-ACDP decreases. In Fig. 9, the mean values of IGD on LIR-CMOP5, 7, 12 and 14 with different values of θ_0 are plotted. We can see that $\theta_0 \in \{\frac{\pi}{2N\times16}, \frac{\pi}{2N\times4}$, and $\frac{\pi}{2N}\}$ have similar performance, and that they are better than those of MOEA/D-ACDP with $\theta_0 > \frac{\pi}{2N}$. Thus, we suggest that θ_0 be set in the interval $[\frac{\pi}{2N\times16}, \frac{\pi}{2N}]$. In this work, θ_0 is set to $\frac{\pi}{2N}$.

5. Conclusions

This paper proposes a new constraint-handling mechanism named ACDP. It utilizes the angle information between any two solutions to dynamically maintain the diversity of the population during the evolutionary process. The proportion of feasible solutions is also used to maintain a balance between convergence and feasibility of a population. A set of CMOP instances called LIR-CMOP1-14 are tested. All the test instances have large infeasible regions in their objective spaces, which make it difficult for many CMOEAs to achieve the real PFs. Compared with the other six popular CMOEAs, the proposed algorithm can help the population to cross large infeasible regions more effectively. Additionally, the experimental results demonstrate that the proposed algorithm can work well on a real-world engineering problem. Thus, we can conclude that MOEA/D-ACDP outperforms the other six CMOEAs. In summary, MOEA/D-ACDP has following advantages:

- The proposed MOEA/D-ACDP utilizes the angle information between solutions to maintain the diversity of the population for CMOPs.
- MOEA/D-ACDP enhances convergence to the PF by exploring feasible and infeasible regions simultaneously during the evolutionary process, instead of wasting the useful information represented by infeasible solutions.

Although the proposed MOEA/D-ACDP performs well on CMOPs with two and three objectives, we still need to enhance its capability for solving CMOPs with more than three objectives. One aspect of our future work is to study the characteristics of constrained optimization problems beyond three objectives, and to design suitable constraint-handling mechanisms in the framework of MOEA/D-ACDP to solve them. Additional planned future work will focus on developing new mechanisms of mining more useful information during the evolutionary process to further improve the performance of the proposed algorithm.

Acknowledgments

This research work was supported by the Key Lab of Digital Signal and Image Processing of Guangdong Province, the National Natural Science Foundation of China under Grant (61175073, 61300159, 61332002, 51375287), the Natural Science Foundation of Jiangsu Province of China under grant SBK2018022017, China Postdoctoral Science Foundation under grant 2015M571751, the Project of International, as well as Hongkong, Macao&Taiwan Science and Technology Cooperation Innovation Platform in Universities in Guangdong Province (2015KGJH2014), and the National Defense Technology Innovation Special Zone Projects (18-163-11-ZT-003-008-01, 18-163-11-ZT-003-008-02).

References

[1] K. Deb, A. Pratap, S. Agarwal, T. Meyarivan, A fast and elitist multiobjective genetic algorithm: NSGA-II, IEEE Trans. Evol. Comput. 6 (2) (2002) 182–197.
[2] N. Srinivas, K. Deb, Muiltiobjective optimization using nondominated sorting in genetic algorithms, Evol. Comput. 2 (3) (1994) 221–248.
[3] T. Murata, H. Ishibuchi, MOGA: Multi-objective genetic algorithms, in: Evolutionary Computation, 1995, IEEE International Conference on, vol. 1, IEEE, 1995, p. 289.
[4] E. Zitzler, L. Thiele, Multiobjective evolutionary algorithms: a comparative case study and the strength pareto approach, IEEE Trans. Evol. Comput. 3 (4) (1999) 257–271.
[5] D.W. Corne, N.R. Jerram, J.D. Knowles, M.J. Oates, PESA-II: region-based selection in evolutionary multiobjective optimization, in: Conference on Genetic and Evolutionary Computation, 2001, pp. 283–290.
[6] E. Zitzler, M. Laumanns, L. Thiele, et al., SPEA2: Improving the Strength Pareto Evolutionary Algorithm, Tik-Report, 2001.
[7] J. Horn, N. Nafpliotis, D.E. Goldberg, A niched pareto genetic algorithm for multiobjective optimization, in: Evolutionary Computation, 1994. IEEE World Congress on Computational Intelligence., Proceedings of the First IEEE Conference on, vol. 1, 2002, pp. 82–87.
[8] Q. Zhang, H. Li, MOEA/D: A multiobjective evolutionary algorithm based on decomposition, IEEE Trans. Evol. Comput. 11 (6) (2007) 712–731.
[9] H. Li, Q. Zhang, Multiobjective optimization problems with complicated Pareto sets, MOEA/D and NSGA-II, IEEE Trans. Evol. Comput. 13 (2) (2009) 284–302.
[10] H.L. Liu, F. Gu, Q. Zhang, Decomposition of a multiobjective optimization problem into a number of simple multiobjective subproblems, IEEE Trans. Evol. Comput. 18 (3) (2014) 450–455.
[11] X. Cai, Y. Li, Z. Fan, Q. Zhang, An external archive guided multiobjective evolutionary algorithm based on decomposition for combinatorial optimization, IEEE Trans. Evol. Comput. 19 (4) (2015) 508–523.
[12] X. Cai, Z. Yang, Z. Fan, Q. Zhang, Decomposition-based-sorting and angle-based-selection for evolutionary multiobjective and many-objective optimization, IEEE Trans. Cybern. PP (99) (2016) 1–14.

[13] E. Zitzler, S. Künzli, Indicator-based selection in multiobjective search, Lecture Notes in Comput. Sci. 3242 (2004) 832–842.
[14] N. Beume, B. Naujoks, M. Emmerich, SMS-EMOA: Multiobjective selection based on dominated hypervolume, European J. Oper. Res. 181 (3) (2007) 1653–1669.
[15] J. Bader, E. Zitzler, HypE: an algorithm for fast hypervolume-based many-objective optimization., Evol. Comput. 19 (1) (2011) 45.
[16] S. Jiang, J. Zhang, Y.-S. Ong, A.N. Zhang, P.S. Tan, A simple and fast hypervolume indicator-based multiobjective evolutionary algorithm, IEEE Trans. Cybern. 45 (10) (2015) 2202–2213.
[17] C.A.C. Coello, A.D. Christiansen, MOSES: A multiobjective optimization tool for engineering design, Eng. Optim. 31 (3) (1999) 337–368.
[18] K. Deb, An efficient constraint handling method for genetic algorithms, Comput. Methods Appl. Mech. Eng. 186 (2) (2000) 311–338.
[19] D. Powell, M.M. Skolnick, Using genetic algorithms in engineering design optimization with non-linear constraints, in: International Conference on Genetic Algorithms, 1993, pp. 424–431.
[20] F. Jimenez, A.F. Gómez-Skarmeta, G. Sánchez, K. Deb, An evolutionary algorithm for constrained multi-objective optimization, in: Evolutionary Computation, 2002. CEC'02. Proceedings of the 2002 Congress on, vol. 2, IEEE, 2002, pp. 1133–1138.
[21] N. Young, Blended ranking to cross infeasible regions in constrainedmultiobjective problems, in: Computational Intelligence for Modelling, Control and Automation, 2005 and International Conference on Intelligent Agents, Web Technologies and Internet Commerce, International Conference on, vol. 2, IEEE, 2005, pp. 191–196.
[22] H.K. Singh, A. Isaacs, T. Ray, W. Smith, Infeasibility driven evolutionary algorithm (IDEA) for engineering design optimization, in: Australasian Joint Conference on Artificial Intelligence, Springer, 2008, pp. 104–115.
[23] T.P. Runarsson, X. Yao, Stochastic ranking for constrained evolutionary optimization, IEEE Trans. Evol. Comput. 4 (3) (2000) 284–294.
[24] T. Takahama, S. Sakai, Efficient constrained optimization by the ε constrained rank-based differential evolution, in: Evolutionary Computation, CEC, 2012 IEEE Congress on, IEEE, 2012, pp. 1–8.
[25] M. Asafuddoula, T. Ray, R. Sarker, K. Alam, An adaptive constraint handling approach embedded MOEA/D, in: Evolutionary Computation, 2012, pp. 1–8.
[26] W. Ning, B. Guo, Y. Yan, X. Wu, J. Wu, D. Zhao, Constrained multi-objective optimization using constrained non-dominated sorting combined with an improved hybrid multi-objective evolutionary algorithm, Eng. Optim. 49 (10) (2017) 1645–1664.
[27] Y.G. Woldesenbet, G.G. Yen, B.G. Tessema, Constraint handling in multiobjective evolutionary optimization, IEEE Trans. Evol. Comput. 13 (3) (2009) 514–525.
[28] M.A. Jan, Q. Zhang, MOEA/D for constrained multiobjective optimization: Some preliminary experimental results, in: 2010 UK Workshop on Computational Intelligence, UKCI.
[29] Y. Wang, Z. Cai, Y. Zhou, W. Zeng, An adaptive tradeoff model for constrained evolutionary optimization, IEEE Trans. Evol. Comput. 12 (1) (2008) 80–92.
[30] B.Y. Qu, P.N. Suganthan, Constrained multi-objective optimization algorithm with an ensemble of constraint handling methods, Eng. Optim. 43 (4) (2011) 403–416.
[31] K. Miettinen, Nonlinear multiobjective optimization, in: International Series in Operations Research and Management Science, vol. 12, Kluwer Academic Publishers, Dordrecht, 1999.
[32] M.A. Jan, R.A. Khanum, A study of two penalty-parameterless constraint handling techniques in the framework of MOEA/D, Appl. Soft Comput. 13 (1) (2013) 128–148.
[33] Z. Yang, X. Cai, Z. Fan, Epsilon constrained method for constrained multiobjective optimization problems: some preliminary results, in: Companion Publication of the 2014 Conference on Genetic and Evolutionary Computation, 2014, pp. 1181–1186.
[34] T. Takahama, S. Sakai, Constrained optimization by the ε constrained differential evolution with gradient-based mutation and feasible elites, in: Evolutionary Computation, 2006. CEC 2006. IEEE Congress on, 2006, pp. 1–8.
[35] Y. Xiang, Y. Zhou, M. Li, Z. Chen, A vector angle-based evolutionary algorithm for unconstrained many-objective optimization, IEEE Trans. Evol. Comput. 21 (1) (2017) 131–152.
[36] R. Cheng, Y. Jin, M. Olhofer, B. Sendhoff, A reference vector guided evolutionary algorithm for many-objective optimization, IEEE Trans. Evol. Comput. 20 (5) (2016) 773–791.
[37] Z. Fan, W. Li, X. Cai, H. Li, K. Hu, Q. Zhang, K. Deb, E.D. Goodman, Difficulty adjustable and scalable constrained multi-objective test problem toolkit, 2016, arXiv preprint arXiv:1612.07603.
[38] Z. Fan, W. Li, X. Cai, H. Huang, Y. Fang, Y. You, J. Mo, C. Wei, E. Goodman, An improved epsilon constraint-handling method in MOEA/D for CMOPs with large infeasible regions, 2017, arXiv preprint arXiv:1707.08767.
[39] S. Huband, P. Hingston, L. Barone, L. While, A review of multiobjective test problems and a scalable test problem toolkit, IEEE Trans. Evol. Comput. 10 (5) (2006) 477–506.
[40] A. Osyczka, Multicriteria optimization for engineering design, in: Design Optimization, 1985, pp. 193–227.
[41] P.A.N. Bosman, D. Thierens, The balance between proximity and diversity in multiobjective evolutionary algorithms, IEEE Trans. Evol. Comput. 7 (2) (2003) 174–188.
[42] Z. Fan, W. Li, X. Cai, H. Li, H. Huang, Z. Cai, An improved epsilon constraint handling method embedded in MOEA/D for constrained multi-objective optimization problems, in: 2016 IEEE Symposium Series on Computational Intelligence, 2016.